

Smartphone-enabled 3D printing of medicines

Xiaoyan Xu¹, Alejandro Manuel Seijo Rabina², Atheer Awad¹, Carlos Rial³, Simon Gaisford^{1,3}, Abdul W. Basit^{1,3,*}, Alvaro Goyanes^{1,2,3,*}

¹ Department of Pharmaceutics, UCL School of Pharmacy, University College London, 29-39 Brunswick Square, London, WC1N 1AX, UK

² Departamento de Farmacología, Farmacia y Tecnología Farmacéutica, I+D Farma (GI-1645), Facultad de Farmacia, and Health Research Institute of Santiago de Compostela (IDIS), Universidade de Santiago de Compostela, 15782 Santiago de Compostela, Spain

³ FabRx Ltd., 7B North Lane, Canterbury, CT2 7EB, UK

*Correspondence: a.basit@ucl.ac.uk (Abdul W. Basit)
a.goyanes@fabrx.co.uk (Alvaro Goyanes)

Abstract

3D printing is a manufacturing technique that is transforming numerous industrial sectors. Within healthcare, it is empowering the small-scale development of personalised medicines that meet the individual needs of patients. 3D printing systems are being currently tested in specialised clinical settings by healthcare professionals, however, there is a need for integrating novel digital solutions that allow for rapid, safe and remote medical interventions directly at the point-of-care. To this end, a portable smartphone-activated 3D printer, operated with a custom mobile app is proposed for the first time to prepare personalised medicines. The printer uses the light from the smartphone's screen to photopolymerise liquid resins and create solid structures. Warfarin-loaded Printlets (3D printed tablets) of various sizes and patient-centred shapes (caplet, triangle, diamond, square, pentagon, torus, and gyroid lattices) were successfully printed in high resolution and dimensional precision using different photosensitive resins. The drug within the Printlets existed in the amorphous form, wherein the Printlets displayed sustained release characterises. The promising proof-of-concept results support the future potential of this compact, user-friendly and interconnected smartphone-based system for point-of-care manufacturing of personalised medications.

Keywords

Three-dimensional printing of drug products; Additive Manufacturing of formulations and drug delivery systems; Personalized Medicines; Digital Healthcare; Printing Pharmaceuticals; Vat photopolymerization

1. Introduction

3D printing is an innovative technology that is changing the way products are manufactured in a range of sectors (Capel et al., 2018). Within healthcare, 3D printers have been particularly transformative, with their ability to print dosage forms on-demand in small production batches (Ragelle et al., 2021), driving the development of personalised medicines and precision treatments (Gioumouxouzis et al., 2019; Karavasili et al., 2021; Prendergast and Burdick, 2020; Uddin et al., 2019), and moving the industry away from the traditional 'one-size-fits-all', large-scale batch manufacture approaches (Aguado et al., 2018). An additional benefit of 3D printing is that it is digital; dosage forms are designed in CAD software and digitised prior to printing (Eleftheriadis et al., 2021a). This digital architecture also means it is relatively straightforward to combine 3D printing manufacture with other cybernated technologies, such as artificial intelligence (AI) (Hirschberg et al., 2020), machine learning (Elbadawi et al., 2020a; Elbadawi et al., 2020b), finite element analysis (Karavasili et al., 2020) and mobile applications (Arden et al., 2021; Muñiz Castro et al., 2021), and it is this combination of digital approaches that really offers the potential to reshape the pharmaceutical landscape.

Because 3D printing enables the fabrication of small batches of medicines with tailored dosages (Eleftheriadis et al., 2021b), sizes, shapes (Melocchi et al., 2019a; Melocchi et al., 2019b), and release profiles (Zheng et al., 2021), it is a viable method for small-scale production of treatments that require customisation and frequent modifications (Elbadawi et al., 2021a; Elbadawi et al., 2021b; Melocchi et al., 2021). This is particularly beneficial for certain drug candidates, such as those with narrow therapeutic indices, those that exhibit high inter-individual pharmacokinetic and pharmacodynamic variabilities, and costly drugs (e.g., cancer and rare disease drugs) (Goyanes et al., 2019; Tyson et al., 2020). Similarly, the disease state and individual patient characteristics (e.g., age, sex, and race) can significantly alter drug product performance, requiring individualised intervention.

3D printing is an overarching term that encompasses a number of technologies, each having its own characteristics and feedstock material requirements (Seoane-Viaño et al., 2021). Of these, vat photopolymerisation-based techniques provide superior printing resolution, high dimensional accuracy, and smooth surface finishes (Ng et al., 2020; Xu et al., 2020a). The process involves a photocuring process, where solid objects are created in a vat of liquid resin under light irradiation. Not originally developed with the healthcare sector in mind, the technology has nevertheless been explored for various

biomedical and pharmaceutical applications, including oral dosage forms (Kadry et al., 2019; Karakurt et al., 2020; Krkobabić et al., 2019; Wang et al., 2016), polypills (Robles-Martinez et al., 2019; Xu et al., 2020b), patient-specific implants and devices (Goyanes et al., 2016; Januszewicz et al., 2020; Vaut et al., 2020; Vivero-Lopez et al., 2021; Xu et al., 2021a; Xu et al., 2021b; Yang et al., 2020), stents (Maity et al., 2021; Paunović et al., 2021), microneedles (Caudill et al., 2021; Caudill et al., 2018; Xenikakis et al., 2021; Xenikakis et al., 2019; Yao et al., 2020), dental splints (Gittard et al., 2011), and functional absorbers (Oh et al., 2019).

The most widely used vat photopolymerisation technologies are stereolithography (SLA), digital light processing (DLP), continuous light interface production (CLIP) and, more recently, liquid crystal display (LCD). The main differences between these technologies lie in the light source and imaging system used (Quan et al., 2020). Whilst SLA uses a laser beam directed by two mirror galvanometers to draw patterns based on the 3D file to selectively cure each layer, DLP and CLIP use a digital light projector, where light is directed using a digital micromirror device (DMD), providing an entire image of a whole layer at once (Tumbleston et al., 2015). LCD 3D printing is also a projection-type technology, but it differs by using light-emitting diode (LED) arrays, which shine through an LCD panel with the screen acting as a mask to create the curing pattern (Madžarević and Ibrić, 2021; Malas et al., 2019).

In recent years, vat photopolymerisation 3D printers based on mobile devices, such as smartphones and tablets, have emerged (e.g., ONO, T3D, LumiBee, Lumifold TB) (Kickstarter, 2021a, b; Li et al.; Lumi Industries, 2021a, b). Like LCD 3D printers, the light from the device's screen is utilised to harden photosensitive resins. In the pharmaceutical field, mobile-based systems may provide a clear benefit to patients who live remotely, improving their accessibility to healthcare by allowing them to obtain their medications directly. Moreover, the interconnectivity of such devices could allow healthcare professionals to monitor the whole preparation process remotely, ensuring patient safety.

Thus, the aim of this proof-of-concept study was to assess the feasibility of utilising a smartphone 3D printer for the fabrication of personalised warfarin sodium Printlets (3D printed tablets) in various geometries. In this work, the suitability of different photopolymer resins and printing parameters was evaluated for the preparation of the Printlets with different doses. The physical properties and release characterisations of the 3D printed formulations were also assessed.

2. Materials and methods

2.1 Materials

Poly(ethylene glycol) diacrylate (PEGDA, average Mn 575 g/mol), Eosin Y disodium salt (EOS, MW 691.85 g/mol), triethanolamine (TEA, MW 149.19 g/mol, $\geq 99.0\%$ (GC),) Tris(2,2'-bipyridyl)dichlororuthenium(II) hexahydrate (Ru), sodium Persulfate (SP), and acetonitrile (ACN, $\geq 99.9\%$, HPLC grade) were purchased from Sigma-Aldrich (Dorset, UK). Riboflavin (RBF, MW 376.37 g/mol, $> 98.0\%$) was obtained from Bio Basic (Toronto, Canada). Warfarin sodium (MW 330.31 g/mol, $\geq 98.0\%$) was acquired from LKT Laboratories Inc. (St. Paul MN, USA). Daylight resin (red, hard) was acquired from RS Components Ltd (Northants, UK). All materials were used as received.

2.2 Emission spectra of the smartphone screen

To facilitate the selection of appropriate photoinitiators, the emission spectra of two smartphones were measured using an Agilent 8453 UV-Vis spectrophotometer (Agilent Technologies, UK) between 200-800 nm. A Huawei P10 mobile phone (Android 7.0) and a Samsung Galaxy A3 (Android 8.0) mobile smartphones were used as models and the emission spectra were collected while the screen displayed a white picture at maximum brightness. The emission spectra of the smartphones were plotted by inverting the absorbance spectra.

2.3 Preparation of drug-loaded photopolymer resins

An initial screening of different visible-light photoinitiators found in the literature was performed to select the most suitable photoinitiator system. Different formulations were prepared with different compositions of photoinitiator, and co-initiator, as shown in **Table 1**. Following the selection of the formulation with optimum printing properties, 5% (w/w) of warfarin sodium was added as model compound. The photopolymer solutions were prepared to a total mass of 5 g in an amber vial, which was magnetically stirred thoroughly at room temperature until the drug was completely dissolved.

Table 1. Different formulations for 3D printing.

Formulation	EOS 1% (w/v) solution (% w/w)	TEA (% w/w)	Ru 1% (w/v) solution (% w/w)	SP 1% (w/v) solution (% w/w)	RBF (% w/w)	Warfarin sodium (% w/w)	PEGDA (% w/w)
RU1			15	47.6			37.4
RBF1		3			0.1		96.9

EOS1	6.92	7.5		85.58
EOS2	6.92	7.5	5	80.58

2.4 Design of Printlets

Printlets (cylindrical) were printed in three sizes; size-8 (8 mm diameter x 2.5 mm height), size-11 (11 mm diameter x 2.5 mm height) and size-16 (16 mm diameter x 2.5 mm height). Dimensions of Printlets in other geometries were designed as caplet (8 mm length x 2.5 mm width x 1.5 mm height), triangle (4 mm radius x 2.5 mm height), diamond (9 mm length x 6.76 mm width x 2.5 mm height), square (8 mm side length x 2.5 mm height), pentagon (4 mm radius x 2.5 mm height), and torus (10 mm outer diameter x 6 mm inner diameter x 2.4 mm height) created with 123D Design (Version 14.2.2, Autodesk Inc., USA). The dimensions of the gyroid lattice Printlets was the same as previously reported with a scale factor of 1.5 (Fina et al., 2018). All the 3D models were exported as stereolithography (.stl) files then loaded into the Chitubox software (China) to slice the 3D models and generate 2D images. The resolution of the projected images was adjusted using the specifications of the smartphone Huawei P10 (Android 7.0) including the screen size (113 x 64 mm) and display resolution (1920 x 1080 pixels) to reflect the original designed dimensions.

2.5 3D Printing process

The smartphone-based printer (M3DIMAKER LUX, FabRx Ltd., UK) (19.5 cm x 19.5 cm x 15 cm) contains a building platform, a resin tank, and a container underneath the resin tank for the smartphone (Figure 1). The resin tank is made of a Teflon™ FEP film, providing maximum transparency. To ensure that the smartphone is in close contact with the printing surface during the printing process, the space underneath the resin tank was set at approximately 1 cm. The previously generated 2D images in Section 2.4 were selected, copied, and pasted into the specific folder on the smartphone for displaying while printing. Then, the prepared photopolymer solution was loaded into the resin tank.

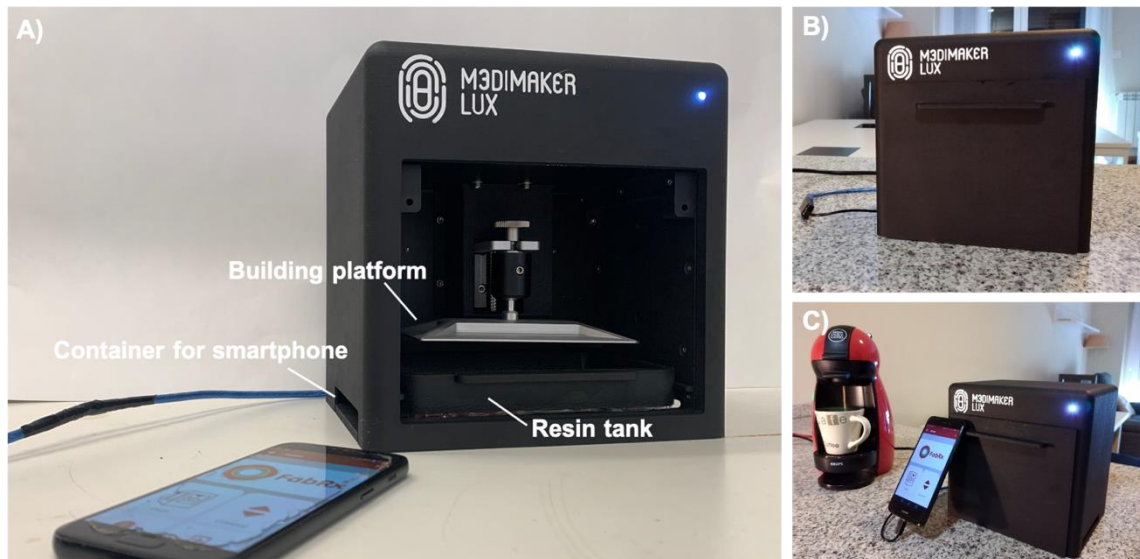


Figure 1. Picture of the A) smartphone-based 3D printer alongside a smartphone, B) the printer with the smartphone inside it during the printing process, and C) comparison of the size of printer with a coffee machine.

A custom printing mobile app was developed to control the printing process of this smartphone-enabled 3D printer. Once connected to a smartphone via a cable, and with the app running, the main menu displays three options, “Print”, “Control”, and “Configuration” (Figure 2). The “Control” page allows the user to control the build platform movement. By clicking the “Configuration” page, different printer settings, including language, z-offset value, up speed, down speed, rise distance, and starting wait time, can be specified. The fabrication of Printlets was initiated by selecting the “Print” page. Some pre-designed 3D models of Printlets with diverse shapes (such as torus, caplet, and square) are displayed in the gallery for patients to choose from. After selecting the desired shape, two printing parameters (exposure time (s) and the layer height (mm)) are selected. In this work, the exposure time was 150 s (60 s for Daylight resin) and the layer height was 0.05 mm. After clicking PRINT, a summary of the printing information with all the selected parameters is displayed for double checking; then the START PRINTING command is selected and the smartphone is returned to the container for the printing process. After printing, the Printlets were gently removed and washed with isopropyl alcohol for 1 min in a sonicator to remove any uncured resin on the surface and post cured for 30 min in a Form Cure (Formlabs Inc., USA). Isopropyl alcohol was selected as it has previously shown to be effective at washing away the unreacted monomers in a short time span (Vivero-Lopez et al., 2021).

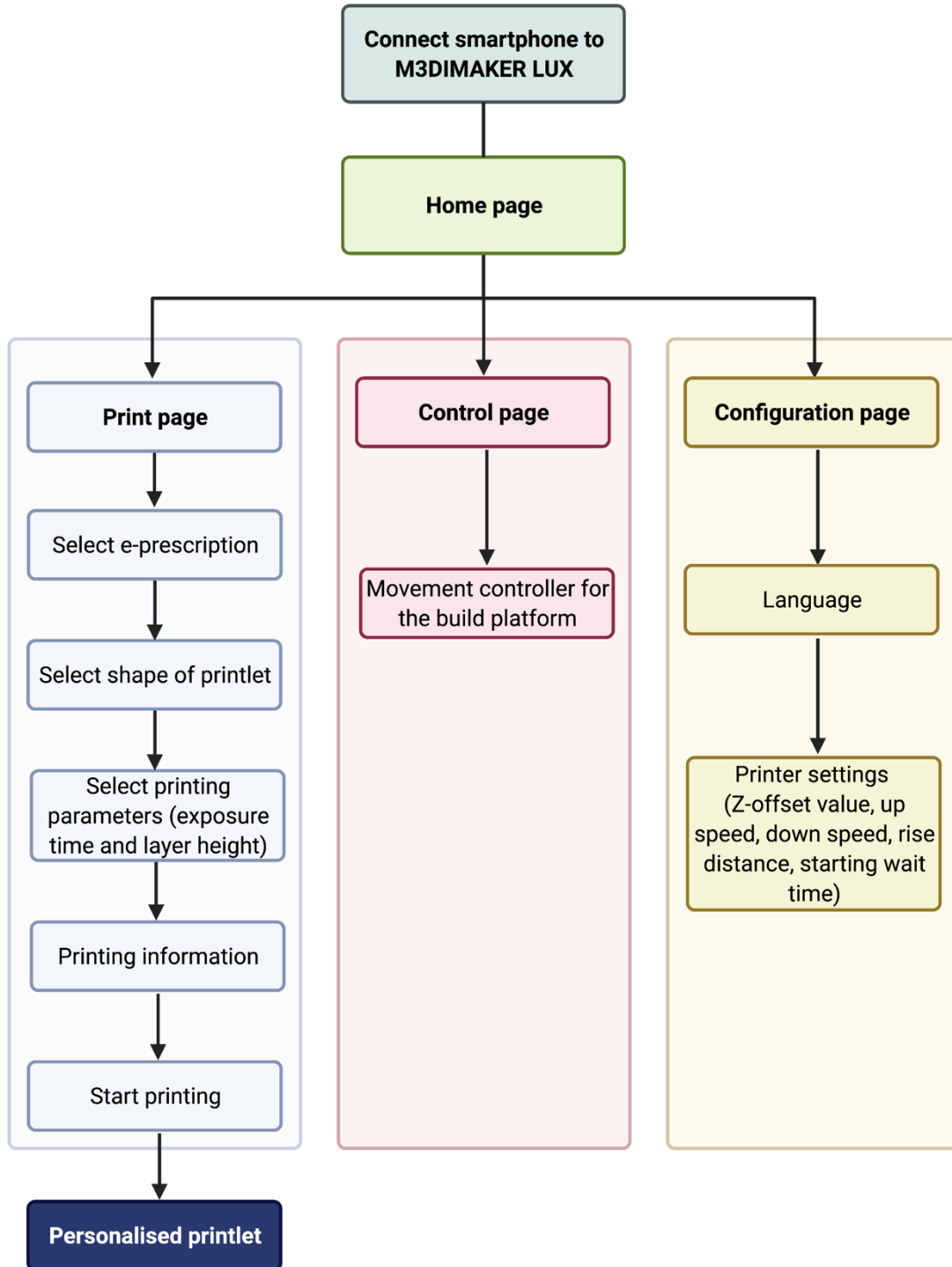


Figure 2. Flow chart of a smartphone-enabled 3D printing process using the custom mobile printing app.

2.6 UV-visible spectrometry

The visible-light photoinitiators including EOS, Ru, and RBF were dissolved in distilled water at concentrations of 0.001% (w/v) for EOS and Ru and 0.004% (w/v) for RBF,

respectively. UV-visible spectra were collected via a Cary 100 UV-Vis spectrophotometer (Agilent Technologies, UK) between 200-800 nm at a scan rate of 600 nm/min.

2.7 Printlet characterisation

2.7.1 Determination of Printlet morphology

The diameter and thickness of the Printlets were measured using a digital calliper (n=3). Images of the Printlets were taken with an iPhone XS (Apple, USA).

2.7.2 X-ray powder diffraction (XRPD)

3D printed drug-loaded discs (23 mm diameter × 1 mm height) were analysed alongside the pure drug (warfarin sodium) powder. X-ray powder diffraction patterns were obtained using a Rigaku MiniFlex 600 (Rigaku, USA) equipped with a Cu K α X-ray source ($\lambda = 1.5418 \text{ \AA}$). The angular range of data acquisition was $3\text{--}60^\circ 2\theta$ with a stepwise size of 0.02° at a speed of $5^\circ/\text{min}$. The intensity and voltage applied were 15 mA and 40 kV, respectively.

2.7.3 Thermal Analysis

Differential scanning calorimetry (DSC) was used to characterise the single drug-loaded printed formulations and the pure drug samples. DSC measurements were performed with a Q2000 DSC (TA instruments, Waters, LLC, USA) at a heating rate of $10^\circ\text{C}/\text{min}$. Calibrations for cell constant and enthalpy were performed with indium ($T_m=156.6^\circ\text{C}$, $\Delta H_f=28.71 \text{ J/g}$) according to the manufacturer instructions. Nitrogen, at a flow rate of $50 \text{ mL}/\text{min}$, was used as a purge gas for all the experiments. Data were collected with TA Advantage software for Q series (Version 2.8.394, TA instruments, Waters, LLC, USA) and analysed using TA Instruments Universal Analysis 2000 (TA instruments, Waters, LLC, USA). All melting temperatures are reported as extrapolated onset, unless otherwise stated. TA aluminium pans and pin-holed hermetic lids (Tzero) were used with an average sample mass of $3\text{--}5 \text{ mg}$.

2.7.4 Scanning electron microscopy (SEM)

The Printlet samples were cut in half, attached to a self-adhesive carbon disc mounted on a 25 mm aluminium stub and coated with 25 nm of gold using a sputter coater. The stub was then placed inside a FEI Quanta 200 FEG Scanning Electron Microscope (FEI, UK) at 5 kV accelerating voltage using secondary electron detection to obtain the cross-section images.

2.7.5 Fourier-Transform infrared spectroscopy (FTIR)

Infrared spectra were collected using a Spectrum 100 FTIR spectrometer (PerkinElmer, Waltham, MA). Warfarin sodium powder and PEGDA were measured as the references. EOS2 photopolymer solution, EOS2 Printlet, and a blank Printlet were scanned over a range of 4000 – 650 cm^{-1} at a resolution of 1 cm^{-1} for 6 scans.

2.8 Determination of drug content in the photopolymer resins and Printlets

Printlets were crushed into fine particles using a mortar and a pestle and dissolved in distilled water contained in volumetric flasks (100 mL) (n=3). The solutions were filtered through a 0.45 μm filter (Merck Millipore Ltd., Ireland) and the concentration of drug was then determined using HPLC (Hewlett Packard 1260 Series HPLC system, Agilent Technologies, Cheshire, UK). An Eclipse plus C18 column, 150 mm \times 4.6 mm (Zorbax, Agilent Technologies, Cheshire, UK) was used as the stationary phase. The mobile phase consisted of 50 mM acetate buffer (pH 5.5) and ACN which was pumped at a flow rate of 1 mL/min under the gradient program as follows: 15 % (v/v) ACN increased to 60 % (v/v) in 5 min and decreased to 15 % (v/v) in 1 min and held for 4 min prior to the next injection. The sample injection volume was 10 μL and the total run time was 10 min, wherein the temperature was set at 30 $^{\circ}\text{C}$ and the eluents were screened at a wavelength of 300 nm.

2.9 Dissolution testing conditions

Dissolution profiles for each type of Printlets were obtained using USP-II apparatus (Model PTWS, Pharmatest, Germany) (n=3). Printlets were first placed in 750 mL of 0.1M HCl (pH 1.2) for 2 h to simulate gastric residence time and then transferred into 950 mL of physiological bicarbonate buffer (Hanks buffer) (pH 5.6–7) for 35 min followed by 1000 mL of modified Krebs buffer (pH 7–7.4 and then to 6.5). Hanks buffer (0.441 mM KH_2PO_4 , 0.337 mM $\text{Na}_2\text{HPO}_4 \cdot 2\text{H}_2\text{O}$, 136.9 mM NaCl, 5.37 mM KCl, 0.812 mM $\text{MgSO}_4 \cdot 7\text{H}_2\text{O}$, 1.26 mM $\text{CaCl}_2 \cdot 2\text{H}_2\text{O}$, 4.17 mM NaHCO_3) was modified to form an in-situ modified Krebs's buffer by the addition of 50 mL of pre-Krebs solution (6.9 mM KH_2PO_4 and 400.7 mM NaHCO_3) to every dissolution vessel (Fadda and Basit, 2005; Goyanes et al., 2015a).

The Printlets were tested in the small intestinal environment for 3.5 h with a pH value of 5.6–7.4, followed by the increase of the pH to 6.5 to simulate the colonic environment (Fadda and Basit, 2005; Goyanes et al., 2015a). The dissolution medium was primarily composed of a bicarbonate buffer system in which both, bicarbonate (HCO_3^-) and

carbonic acid (H_2CO_3), co-existed in equilibrium with the CO_2 (aq) generated from the dissociation of the carbonic acid (Goyanes et al., 2015a). The pH of the bicarbonate buffer was modulated and controlled using an Auto pH System™ which incorporates a pH probe connected to a supply of CO_2 (pH-reducing gas) and helium (pH-increasing gas) (Merchant et al., 2014). During dissolution testing, the control unit monitored the pH changes and dynamically adjusted the pH values by pumping CO_2 or helium into the dissolution vessels.

The paddle speed of the USP-II was fixed at 50 rpm and the dissolution medium was maintained at 37 ± 0.5 °C. 1 mL samples were withdrawn from each vessel every half an hour in the first 3 h, followed by every hour. The percentage of drug released from the Printlets was determined using HPLC (previously described in section 2.8).

3. Results and discussions

For the first time, a smartphone-enabled 3D printer was tested for the fabrication of personalised medications (Figure 1). Herein, the light from the smartphone screen was utilised as the illumination source to irradiate the designed patterns and generate physical objects by solidifying the photoreactive materials above the smartphone in the resin tank. The printing process can be easily activated and directly controlled via a built-in custom mobile app, which enables the control of various printing parameters including the exposure time and layer resolution. Besides, the use of visible light is considered a safer fabrication process over ultraviolet (UV) light used in some of the commercial SLA or DLP 3D printers, offering the benefits of reduced risk of eye damage and improved biocompatibility and functional group tolerance (Ahn et al., 2020; Park et al., 2018).

To enable the selection of the most suitable photoinitiator, the spectral power distribution of the smartphone display was measured (Figure 3). The smartphone showed its emission spectrum within the visible spectrum with spikes showing at the blue, green, and red regions. Although the emission spectrum of most of the smartphone is expected to be similar, the intensity may vary between different smartphones. This however can be accounted for by adjusting the exposure time on the printing software based on the model/type of smartphone used to operate the printer.

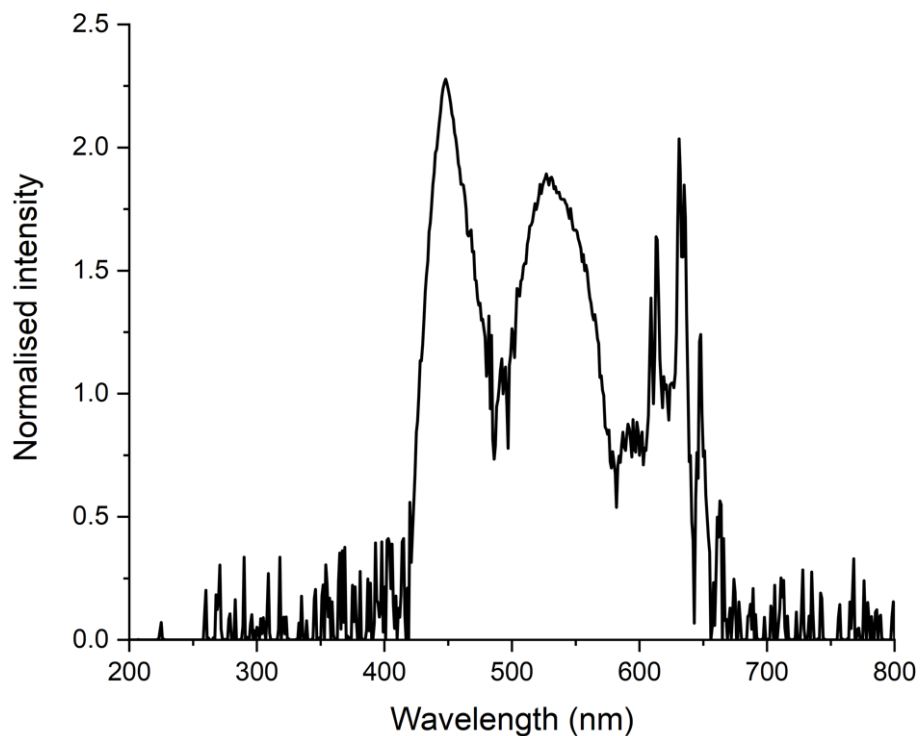


Figure 3. Emission spectra of the smartphone screen showing a white background with 100% screen brightness (Huawei P10, Android 7.0).

Several visible-light photoinitiators found in the literature were examined by measuring their absorption spectra in the visible light range (Figure 4). Eosin Y (EOS) is a xanthene dye commonly used for histological staining, which shows absorbance at 500-520 nm (Freire et al., 2014; Shih and Lin, 2013). Recently, a new visible-light photoinitiating system containing tris (2'2-bipyridyl) dichlororuthenium (II) hexahydrate (Ru) and sodium persulfate (SPS) has been developed for radical polymerisation (350-450 nm) (Lim et al., 2016). Likewise, riboflavin (RBF) also known as vitamin B2, has been widely applied as a visible-light non-toxic photoinitiator, possessing absorbance maxima between 350-450 nm (Ahmad et al., 2013; Madžarević and Ibrić, 2021).

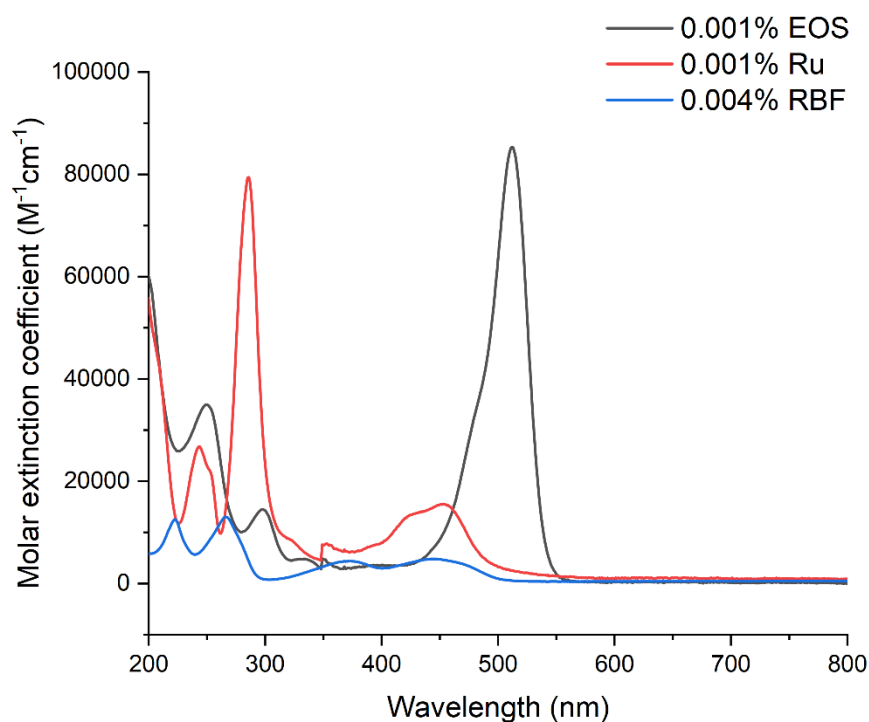


Figure 4. UV-vis spectra for 0.001% (w/v) EOS, 0.001% (w/v) Ru, and 0.004% (w/v) RBF in distilled water.

In the initial screening, each of the visible-light photoinitiators and their co-initiators were incorporated in the photopolymer solution containing PEGDA and loaded into the printer. Under an exposure time of 120 s per layer, EOS1 (Figure 5A) and RU1 (Figure 5B) Printlets were successfully obtained. EOS1 Printlets exhibited better printability and higher dimensional accuracy compared to RU1 Printlets. All the Printlets had an orange colour attributed to the presence of Eosin Y. Unfortunately, no Printlets could be obtained from the riboflavin-based formulation (RBF1) even with a longer exposure time of up to 350s per layer. Therefore, EOS1 was selected as the base formulation used for subsequent printing with the model drug, warfarin sodium.

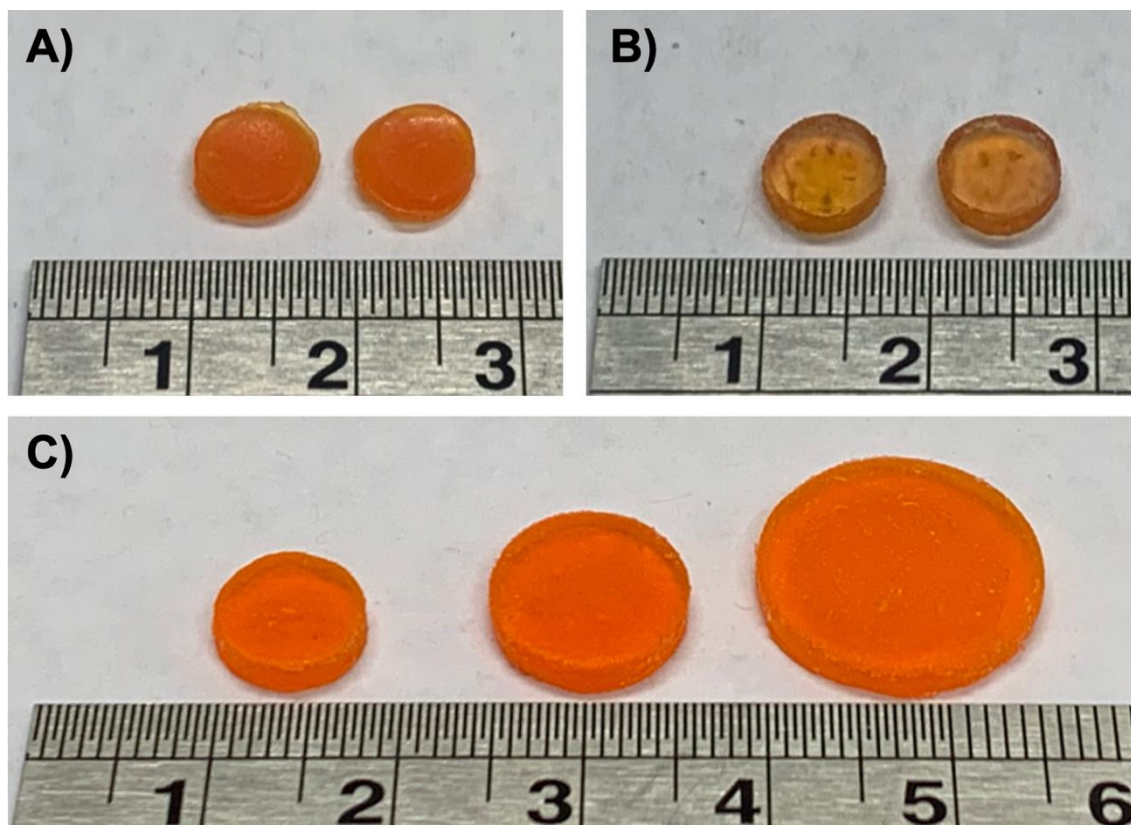


Figure 5. Photographs of A) EOS1 size-8 Printlets, B) RU1 size-8 Printlets and C) EOS2 (from left to right) size-8, size-11, and size-16 Printlets. Scale shown in cm.

Warfarin-loaded Printlets (EOS2) in three different sizes were designed and successfully prepared (Figure 5C). Similar to the EOS1 printlets, all EOS2 Printlets had the same orange colour. SEM images showed that all Printlets were fabricated with flat and smooth outer surfaces (Figure 6), wherein the layer-by-layer feature of 3D printing was recognised in **Figure 6C**. Additionally, the reduced size of the resin tank (14.5 cm x 8.5 cm x 2 cm) and the build platform (12.5 cm x 6.5 cm) (Supplementary Figure A) compared to commercial DLP 3D printers could be advantageous for cost and material saving purposes. As observed in **Supplementary Figure A**, multiple Printlets could be prepared at the same time in 2 h 20 min, suggesting the potential and convenience of this novel platform in preparing small batches of personalised medicines overnight. The average diameter, thickness, and weight of different EOS2 Printlets are shown in **Table 2**. All the Printlets were fabricated with uniform diameter and thickness as designed, highlighting the high resolution and precision of this printing system.

Warfarin is a widely prescribed oral anticoagulant for the treatment and prevention of thromboembolic disorders. Due to its narrow therapeutic index and large variability in interpatient response, the safe use of warfarin sodium is challenging (Kimmel, 2008;

Reynolds et al., 2007). In particular, because it is commercially available in a limited number of doses (0.5, 1, 3, 4, and 5 mg) (BNF, 2021), achieving specific doses requires the patient to take a combination of tablets or to split large-dose tablets. This is clearly unsatisfactory, increasing the risk of medication non-adherence and dosing errors, potentially leading to unwanted adverse events and/or subsequent hospitalisations (Vuddanda et al., 2018). Therefore, the use of warfarin sodium could be safeguarded by dispensing tablets with doses individualised for each patient (Niese et al., 2019).

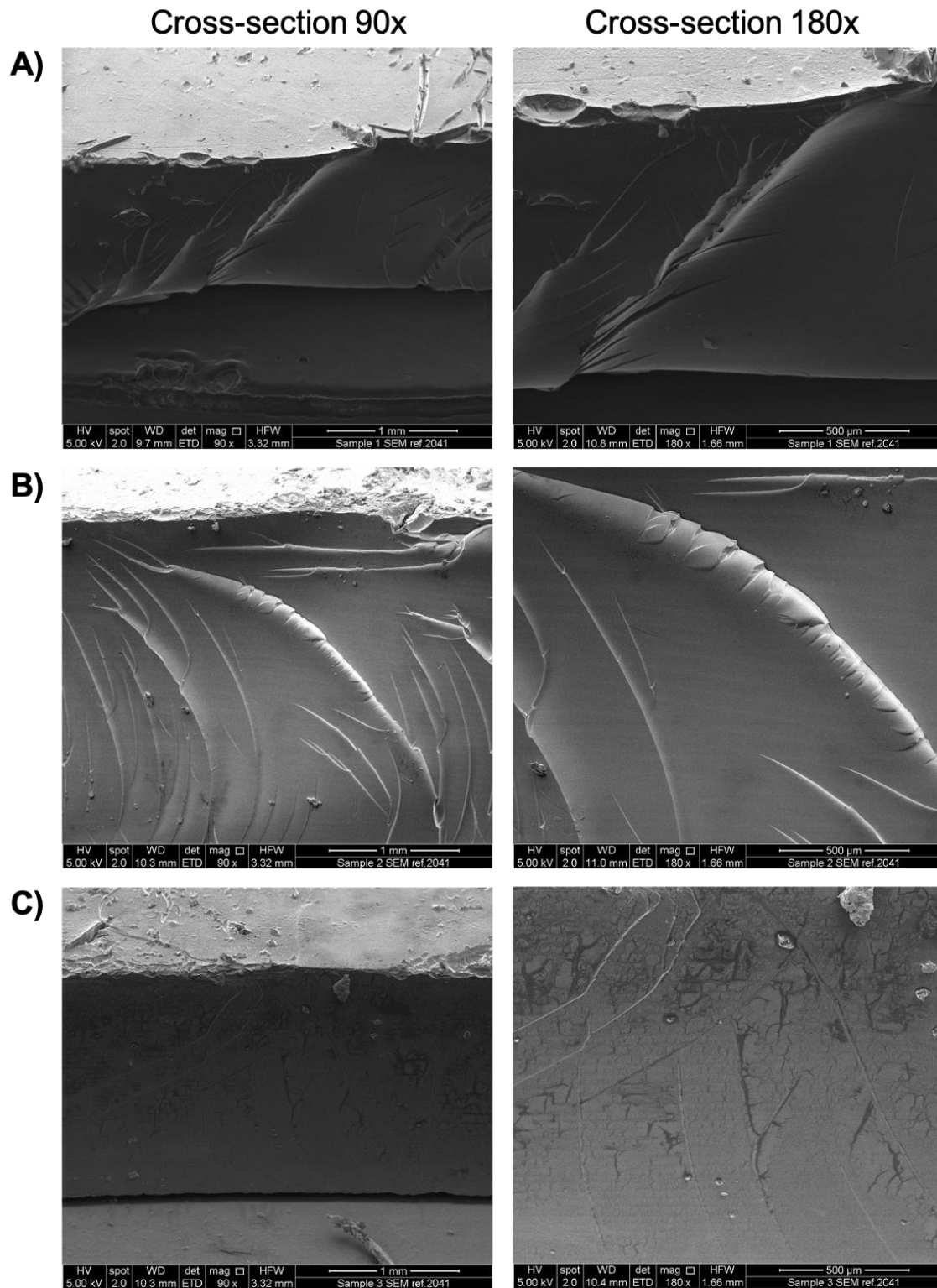


Figure 6. SEM images of cross-sections of EOS2 Printlets in A) size-8, B) size-11, and C) size-16.

1

Table 2. Dimensions and drug loading of the EOS2 Printlets

	Diameter (mm)	Deviation in diameter (%)	Thickness (mm)	Deviation in thickness (%)	Weight (mg)	Drug loading (%)	Dose (mg)
Size-8	8.08 ± 0.06	1.00	2.45 ± 0.03	-2.00	148.37 ± 5.45	5.08 ± 0.04	7.54
Size-11	11.07 ± 0.07	0.64	2.48 ± 0.04	-0.80	283.17 ± 1.29	5.05 ± 0.02	14.30
Size-16	16.05 ± 0.10	0.31	2.44 ± 0.03	-2.40	594.43 ± 11.65	4.92 ± 0.04	29.25

2

To demonstrate the flexibility of this smartphone-enabled platform, Printlets with various geometries (Figure 7A) were fabricated using the EOS1 formulations providing benefits for developing patient-centric medicines. Gyroid lattice Printlets (Figure 7B) were prepared using EOS1 formulations as well as commercial hard resin in high resolutions, illustrating the adaptability of this 3D printer to versatile materials.

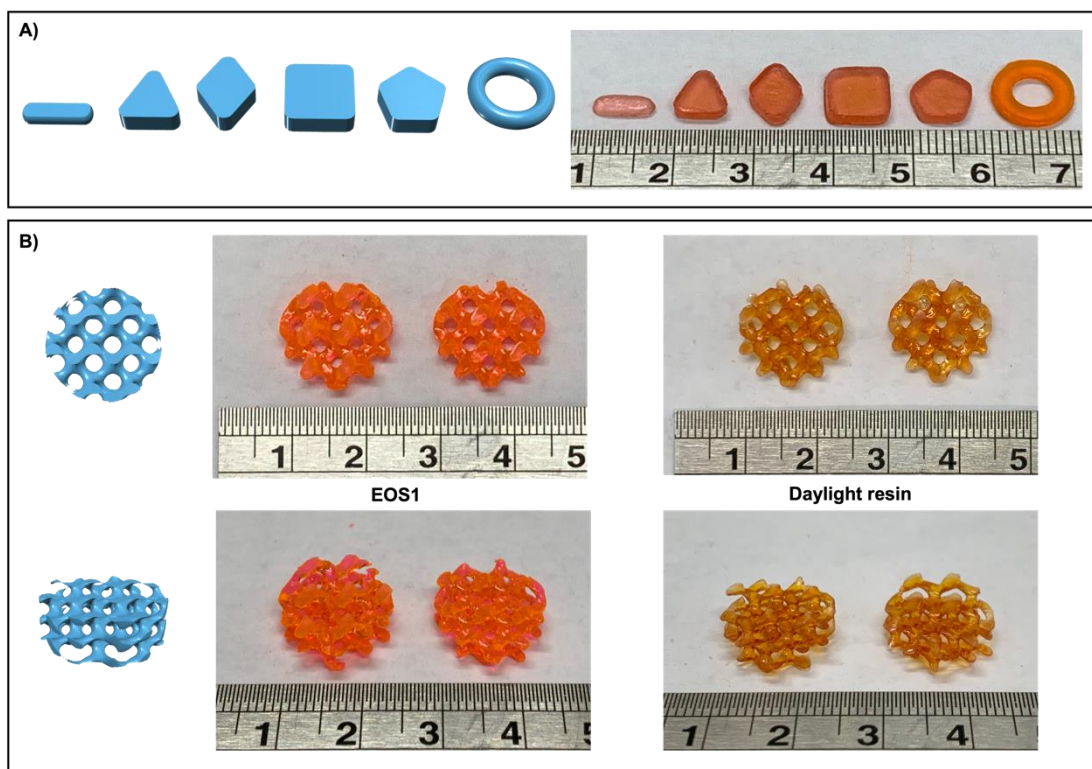


Figure 7. 3D models (left) and photographs (right) of A) EOS1 Printlets in various geometries including (from left to right) caplet, triangle, diamond, square, pentagon, and torus, and B) gyroid lattice Printlets prepared in this study. Scale shown in cm.

Drug loading of Printlets were evaluated using HPLC (Table 2). The theoretical loading of warfarin was selected as 5% (w/w) and all the Printlets were fabricated with drug loadings similar to that value. By varying the diameter of the 3D design, the Printlets were fabricated to incorporate various warfarin doses; 7.54 mg, 14.30 mg, and 29.25 mg for size-8, size-11, and size-16 Printlets, respectively, highlighting the capability of this 3D printing platform in enabling flexible dosing to suit the needs of individual dosing requirements.

XRPD and DSC analyses were performed to investigate the physical state of warfarin sodium in the EOS2 Printlets (Figure 8). The XRPD data (Figure 8A) showed

characteristic peaks of warfarin sodium at 8.1° and 19.2° 2θ , which were not visible in the EOS2 Printlets. The results suggest that the drug is present in an amorphous phase in the printed formulations. Likewise, the DSC thermogram (Figure 8B) displayed a broad endothermic peak at 190°C for pure warfarin (Vuddanda et al., 2018) whereas no melting peak was observed in the Printlet, again suggesting the drug was in the amorphous form in the Printlet.

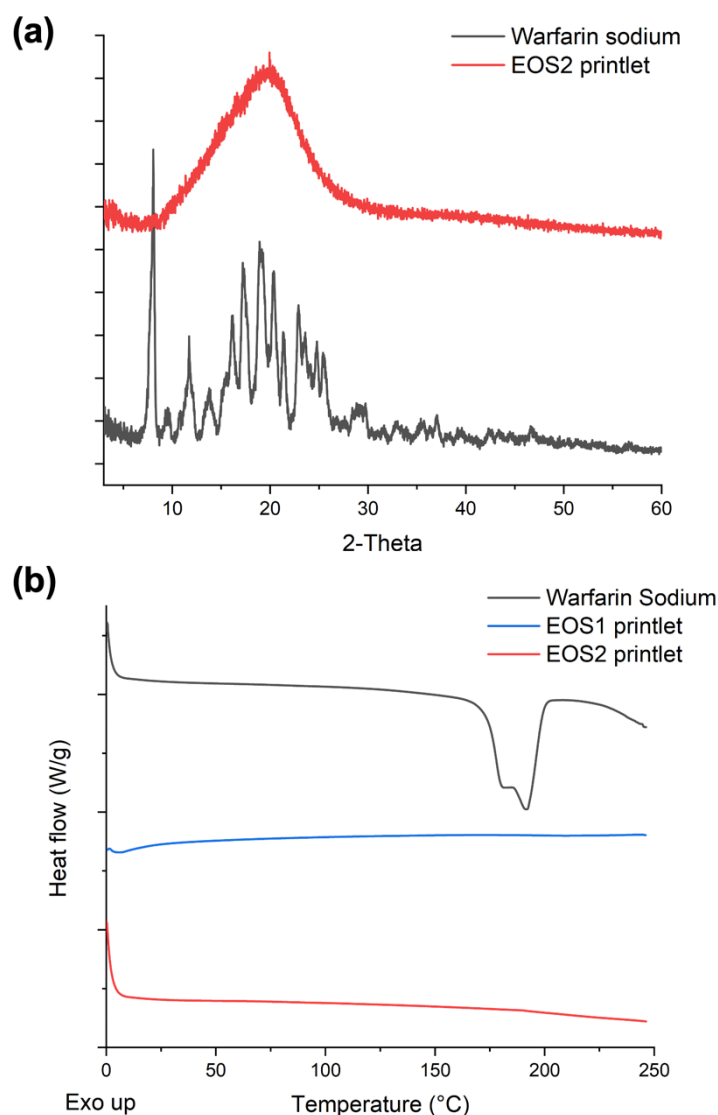


Figure 8. A) X-ray powder diffractograms, and B) DSC thermograms of the pure drug (warfarin sodium), EOS1 Printlet, and EOS2 Printlet.

FTIR spectra (Figure 9) were obtained to investigate the possible drug-photopolymer interactions before and after 3D printing, which has been previously reported during the preparation of oral dosage forms (Xu et al., 2020b). Typical bands of warfarin sodium are seen at $2850\text{-}2950\text{ cm}^{-1}$ (asymmetric CH_2 stretching), 1720 cm^{-1} and 1668 cm^{-1} ($\text{C}=\text{O}$

stretching), 1451 cm^{-1} (asymmetric bending vibrations of CH_3), and 704 cm^{-1} and 758 cm^{-1} (out-of-plane bending vibrations of C-H of phenyl rings) (Parfenyuk and Dolinina, 2017; Vuddanda et al., 2018; Yang and Song, 2015). The characteristic bands were present in the FTIR spectra of EOS2 photopolymer solution and EOS2 Printlet, indicating no drug-photopolymer interactions. As expected, these distinctive peaks were not observed in the blank formulation (EOS1 Printlet). Before the DLP 3D printing process, PEGDA and EOS2 photopolymerisation showed typical acrylate peaks at 1722 cm^{-1} (C=O stretching), 1633 cm^{-1} (C=C stretching), 1408 cm^{-1} and 810 cm^{-1} ($\text{CH}_2=\text{CH}$) (Kadry et al., 2019; Krkobabić et al., 2019), which disappeared in the Printlets (EOS1 and EOS2 Printlets). This observation can be contributed to the conversion of C=C bonds to C-C bonds.

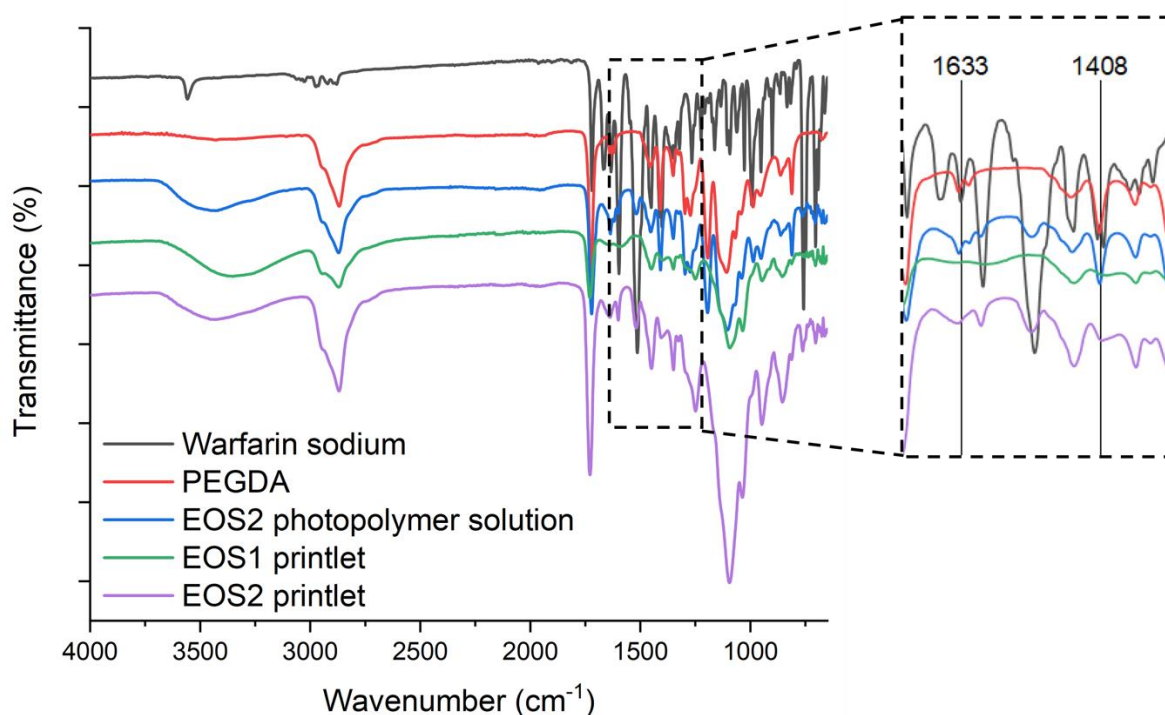


Figure 9. FTIR spectra of warfarin, PEGDA, EOS2 photopolymer solution, EOS1 Printlet (blank), and EOS2 Printlet.

The Printlets were then tested in a dynamic dissolution *in vitro* model, which mimics the gastric and intestinal conditions of the gastrointestinal tract (Figure 10). The release of warfarin commenced slowly in the gastric phase during the first 2 h. This is because warfarin sodium is a weak acid (pK_a 5.05) and exhibits a pH-dependent solubility profile (Nguyenpho et al., 2015). After 2 h, the drug release rates from all Printlets increased in the intestinal phase and continued throughout the remaining 22 h. All the Printlets displayed sustained warfarin release, reaching a release of 79.2%, 71.6%, and 76.1% from the size-8, size-11, and size-16 Printlets after 24 h, respectively. In a previous study,

Printlets with higher surface area to volume ratio demonstrated faster dissolution rates (Goyanes et al., 2015b). Although size-8 Printlets exhibited a higher warfarin release rate, because of their highest surface area to volume (1.32), size-11 (1.16) and size-16 (1.05) Printlets unexpectedly showed similar release profiles. This may be a result of the cracks present on the surface of the Printlets, which were observed after the dissolution study (**Supplementary Figure B**).

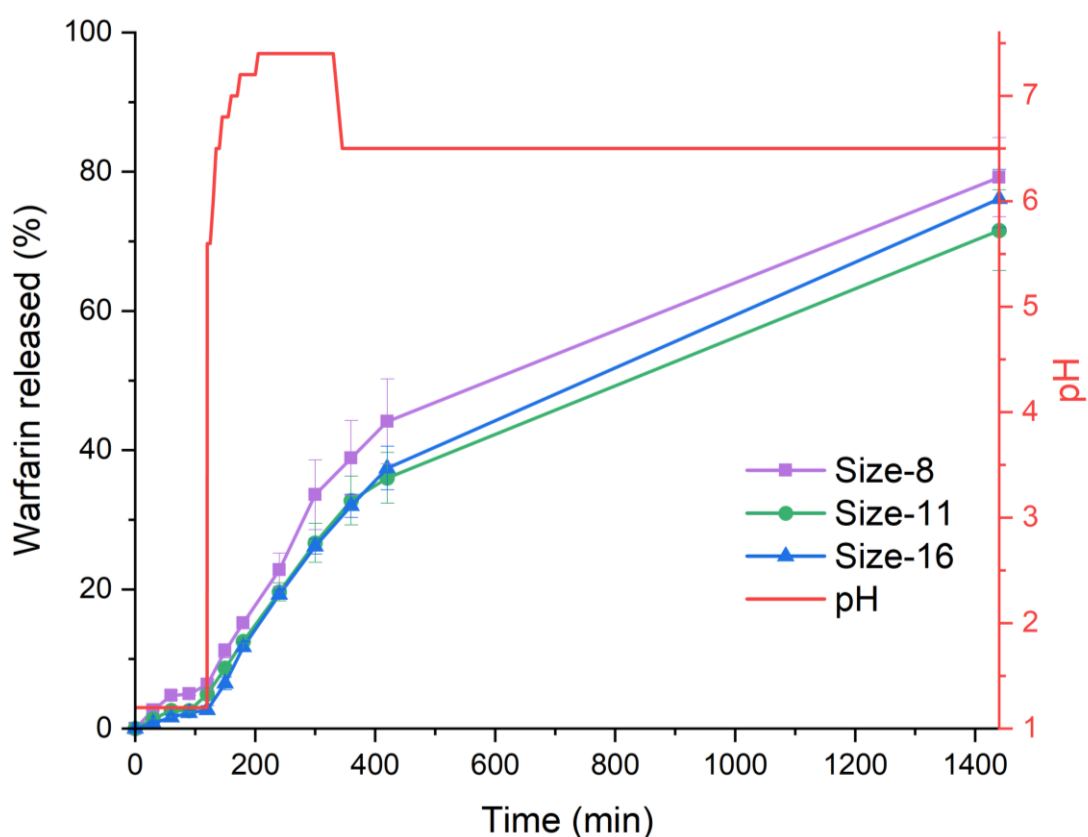


Figure 10. Cumulative release profiles of EOS2 size-8, size-11, and size-16 Printlets. Data values represent mean \pm SD (n=3).

Nowadays, smartphones have become inevitable for daily life activities with their ability to provide access to internet information. Therefore, the smartphone platform has emerged as a promising and cost-effective alternative for serving affordable and accessible healthcare. Although smartphone-based point-of-care applications are increasingly reported, most of them utilise the smartphone's camera for diagnostic and monitoring purposes, or for data collection and analysis through smartphone apps (Kühnemund et al., 2017; Laksanasopin et al., 2015; Mannino et al., 2018). A method for directly fabricating pharmaceuticals using one's own mobile phone could be

advantageous for printing medications at home, on the move or even in resource-limited areas. Herein, we introduce a proof-of-concept utility of a smartphone-based 3D printer for the preparation of warfarin-loaded Printlets. The printer is portable and easy to operate, and the design of the custom printing app is simple, making it suitable for use, even in the absence of professional knowledge on 3D printer operation or 3D model design. Compared with the recently reported DLP 3D printer based on a smartphone-powered pocket projector (Li et al.), the 3D printing platform proposed herein uses the smartphone itself as the light source for controlling the printer as well as generating curing patterns.

This all-in-one system can potentially be integrated in electronic health systems for manufacturing personalised medicines at the point-of-care. Nowadays, with the development of mobile sensing and health monitoring, doctors can remotely manage the patient's medication and provide adjustment of dosages according to the patient's disease condition or pain level. It can be envisioned that, in the future, patients can directly receive their daily electronic prescriptions from doctors or GP practices on their smartphone app with all the information needed including the size of the Printlet for the required doses. Patients could then simply choose the shape of oral dosage form they prefer and by clicking on the prescription, they can eventually print their own medicines overnight at home. In addition, elderly patients can benefit from this system by printing their own polypills to reduce pill burdens. Interestingly, while some might regard this as primitive, the Medicines & Healthcare products Regulatory Agency (MHRA) is in fact currently evaluating individual patient homes as potential point-of-care sites (Medicines & Healthcare products Regulatory Agency, 2021).

The findings of the present study establish a proof-of-concept for the potential of this 3D printing device, however several safety and regulatory concerns should first be addressed to enable its translation into real-world healthcare benefits. A salient drawback is the potential toxicity of resins used in the photopolymerisation process (Oesterreicher et al., 2016; Oskui et al., 2015), which are typically composed of (meth)acrylate-based monomers. In their uncured state, these monomers may leach out from the Printlets, presenting a potential risk for developing allergic reactions or cytotoxicity. Whilst these residual monomers may be removed by post-washing and -curing methods, the equipment needed for this may not be readily available. Therefore, alternative processes or materials freely available at points-of-care should be considered and evaluated instead.

Another challenge is the danger of drug abuse or misuse, potentially risking the lives of individuals. However, this can be avoided by integrating several digital health technologies that safeguard the use of medicines (Awad et al., 2021); this could include designing a system that requires remote approval by a designated healthcare professional, integrating AI technologies to adjust printing parameters so that the final drug product meets the intended therapeutic activity (Elbadawi et al., 2021a; Elbadawi et al., 2021b), and implementing remote drug monitoring and sensing technologies to ensure that patients are adhering to their treatment plan. Additionally, a regulatory framework concerned with 3D printed drug-laden products should be developed, whereby the legislation should counterbalance the potential benefits provided to patients and the safety risks these technologies pose. It is also vital to develop quality control measures that enable the evaluation of the quality of final drug products in a quick, yet non-destructive manner. To ensure that these control measures are being met and implemented correctly, a dedicated hub should oversee the workflow of these individual production sites (Medicines & Healthcare products Regulatory Agency, 2021). While research in the field of 3D printing pharmaceuticals is still nascent, with the correct measures in place and proper framework built, its true potential can be realised sooner rather than later.

4. Conclusion

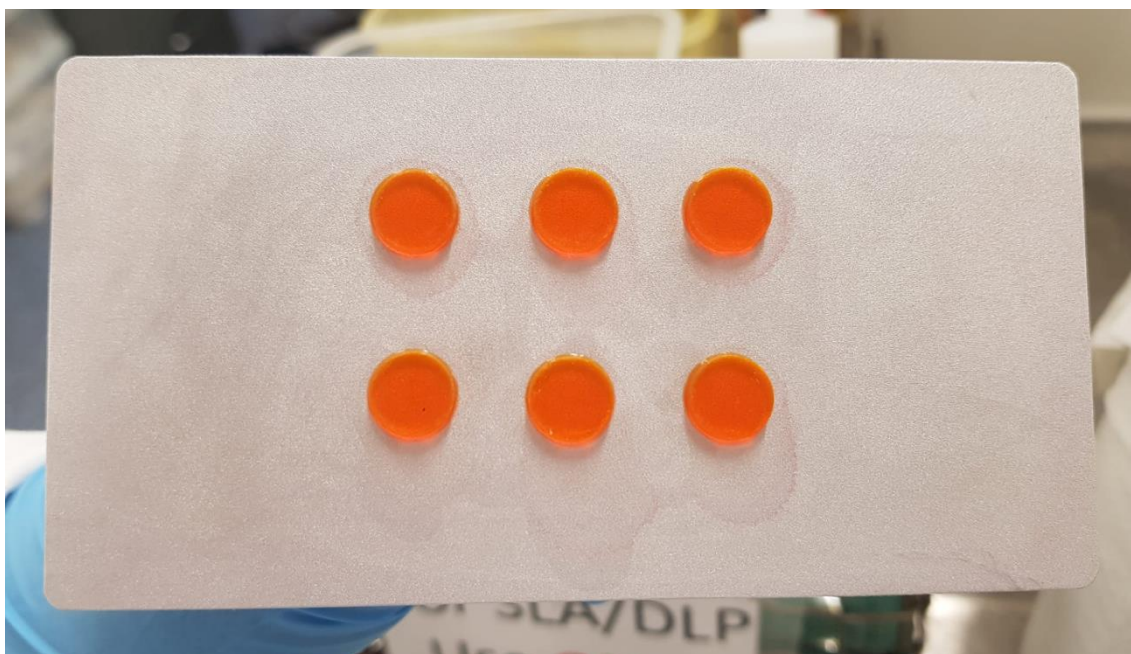
Here, a compact smartphone-based 3D printer and a customised printing app were used for the preparation of Printlets. The light from the screen of a smartphone enabled the direct preparation of personalised medications. Warfarin sodium, a narrow-therapeutic-index drug, was used as the model compound to manufacture oral Printlets with various doses, sizes and shapes with high accuracy and precision.

This 3D printing platform has the potential to be integrated in digital healthcare for point-of-care manufacturing of personalised medicines at a patient's home, in emergency, or resource-limited settings. In the future, this type of system may also possess great significance for achieving a new milestone for affordable and accessible mobile-health technologies. For this to be achieved, several challenges were identified and should be overcome. Additionally, an appropriate regulatory framework must be established, enabling the realisation of the true benefits of a novel healthcare model.

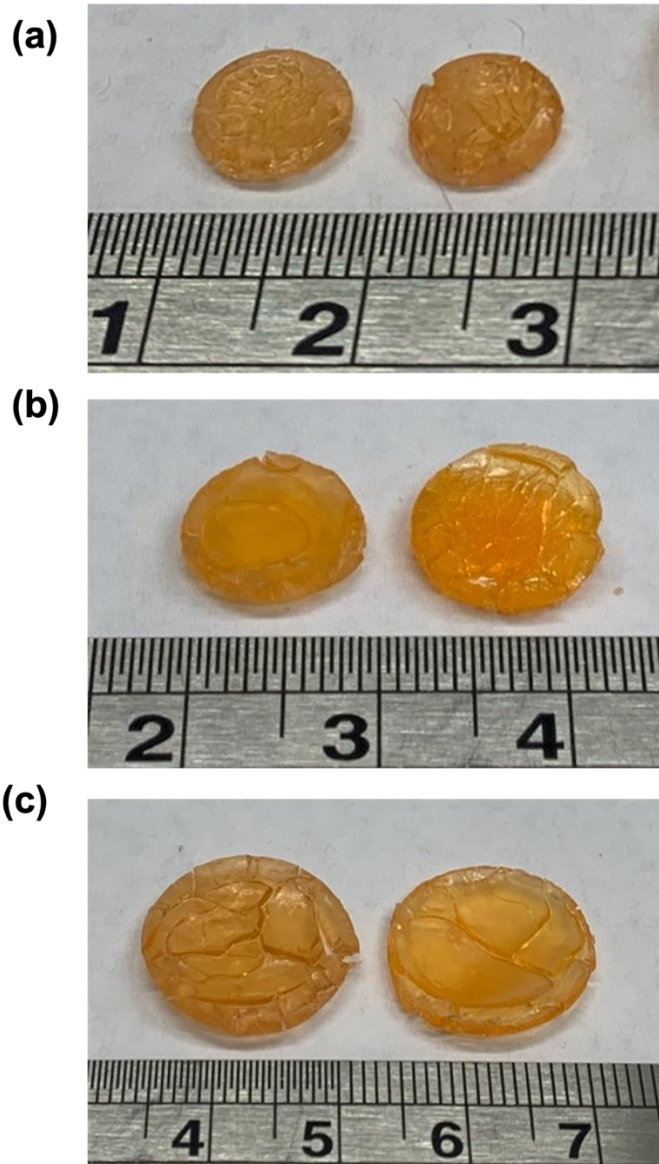
Acknowledgements

The authors thank 3D Limitless for their technical expertise with the development of the 3D printing system, and for their continual support during the study. The graphical abstract and Figure 2 were created with BioRender.com.

Supplementary data



Supplementary Figure A. Photograph of multiple EOS2 size-11 Printlets printed on the build platform of the smartphone-based 3D printer.



Supplementary Figure B. Photograph of EOS2 A) size-8, B) size-11, and C) size-16 Printlets after dissolution test. Scale shown in cm.

References

- Aguado, B.A., Grim, J.C., Rosales, A.M., Watson-Capps, J.J., Anseth, K.S., Engineering precision biomaterials for personalized medicine. *Science translational medicine* **10**, 2018.
- Ahmad, I., Iqbal, K., Sheraz, M.A., Ahmed, S., Mirza, T., Kazi, S.H., Aminuddin, M., Photoinitiated polymerization of 2-hydroxyethyl methacrylate by riboflavin/triethanolamine in aqueous solution: a kinetic study. *ISRN pharmaceuticals* **2013**, 2013.
- Ahn, D., Stevens, L.M., Zhou, K., Page, Z.A., Rapid high-resolution visible light 3D printing. *ACS central science* **6**, 2020, 1555-1563.
- Arden, N.S., Fisher, A.C., Tyner, K., Lawrence, X.Y., Lee, S.L., Kopcha, M., Industry 4.0 for Pharmaceutical Manufacturing: Preparing for the Smart Factories of the Future. *International journal of pharmaceuticals*, 2021, 120554.
- Awad, A., Trenfield, S.J., Pollard, T.D., Jie Ong, J., Elbadawi, M., McCoubrey, L.E., Goyanes, A., Gaisford, S., Basit, A.W., Connected Healthcare: Improving Patient Care using Digital Health Technologies. *Advanced Drug Delivery Reviews*, 2021, 113958.
- BNF, 2021. Warfarin sodium
- Capel, A.J., Rimington, R.P., Lewis, M.P., Christie, S.D.R., 3D printing for chemical, pharmaceutical and biological applications. *Nature Reviews Chemistry* **2**, 2018, 422-436.
- Caudill, C., Perry, J.L., Iliadis, K., Tessema, A.T., Lee, B.J., Mecham, B.S., Tian, S., DeSimone, J.M., Transdermal vaccination via 3D-printed microneedles induces potent humoral and cellular immunity. *Proceedings of the National Academy of Sciences* **118**, 2021.
- Caudill, C.L., Perry, J.L., Tian, S., Luft, J.C., DeSimone, J.M., Spatially controlled coating of continuous liquid interface production microneedles for transdermal protein delivery. *Journal of Controlled Release* **284**, 2018, 122-132.
- Elbadawi, M., Gustaffson, T., Gaisford, S., Basit, A.W., 3D printing tablets: Predicting printability and drug dissolution from rheological data. *Int J Pharm* **590**, 2020a, 119868.
- Elbadawi, M., McCoubrey, L.E., Gavins, F.K.H., Ong, J.J., Goyanes, A., Gaisford, S., Basit, A.W., Disrupting 3D printing of medicines with machine learning. *Trends Pharmacol. Sci.* **42**, 2021a, 745-757.
- Elbadawi, M., McCoubrey, L.E., Gavins, F.K.H., Ong, J.J., Goyanes, A., Gaisford, S., Basit, A.W., Harnessing artificial intelligence for the next generation of 3D printed medicines. *Advanced Drug Delivery Reviews* **175**, 2021b, 113805.
- Elbadawi, M., Muñiz Castro, B., Gavins, F.K.H., Jie Ong, J., Gaisford, S., Pérez, G., Basit, A.W., Cabalar, P., Goyanes, Á., M3DISEEN: A Novel Machine Learning Approach for Predicting the 3D Printability of Medicines. *Int J Pharm* **590**, 2020b, 119837.
- Eleftheriadis, G.K., Genina, N., Boetker, J., Rantanen, J., Modular design principle based on compartmental drug delivery systems. *Advanced Drug Delivery Reviews* **178**, 2021a, 113921.

Eleftheriadis, G.K., Kantarelis, E., Monou, P.K., Andriotis, E.G., Bouropoulos, N., Tzimtzimis, E.K., Tzetzis, D., Rantanen, J., Fatouros, D.G., Automated digital design for 3D-printed individualized therapies. *Int J Pharm* **599**, 2021b, 120437.

Fadda, H.M., Basit, A.W., Dissolution of pH responsive formulations in media resembling intestinal fluids: bicarbonate versus phosphate buffers. *Journal of Drug Delivery Science and Technology* **15**, 2005, 273-279.

Fina, F., Goyanes, A., Madla, C.M., Awad, A., Trenfield, S.J., Kuek, J.M., Patel, P., Gaisford, S., Basit, A.W., 3D printing of drug-loaded gyroid lattices using selective laser sintering. *Int J Pharm* **547**, 2018, 44-52.

Freire, F., Costa, A.C.B.P., Pereira, C.A., Junior, M.B., Junqueira, J.C., Jorge, A.O.C., Comparison of the effect of rose bengal-and eosin Y-mediated photodynamic inactivation on planktonic cells and biofilms of *Candida albicans*. *Lasers in medical science* **29**, 2014, 949-955.

Gioumouxouzis, C.I., Karavasili, C., Fatouros, D.G., Recent advances in pharmaceutical dosage forms and devices using additive manufacturing technologies. *Drug Discov. Today* **24**, 2019, 636-643.

Gittard, S.D., Miller, P.R., Jin, C., Martin, T.N., Boehm, R.D., Chisholm, B.J., Stafslie, S.J., Daniels, J.W., Cilz, N., Monteiro-Riviere, N.A., Deposition of antimicrobial coatings on microstereolithography-fabricated microneedles. *Jom* **63**, 2011, 59-68.

Goyanes, A., Det-Amornrat, U., Wang, J., Basit, A.W., Gaisford, S., 3D scanning and 3D printing as innovative technologies for fabricating personalized topical drug delivery systems. *Journal of controlled release* **234**, 2016, 41-48.

Goyanes, A., Hatton, G.B., Merchant, H.A., Basit, A.W., Gastrointestinal release behaviour of modified-release drug products: Dynamic dissolution testing of mesalazine formulations. *Int J Pharm* **484**, 2015a, 103-108.

Goyanes, A., Madla, C.M., Umerji, A., Duran Piñeiro, G., Giraldez Montero, J.M., Lamas Diaz, M.J., Gonzalez Barcia, M., Taherali, F., Sánchez-Pintos, P., Couce, M.-L., Gaisford, S., Basit, A.W., Automated therapy preparation of isoleucine formulations using 3D printing for the treatment of MSUD: First single-centre, prospective, crossover study in patients. *Int J Pharm* **567**, 2019, 118497.

Goyanes, A., Robles Martinez, P., Buanz, A., Basit, A.W., Gaisford, S., Effect of geometry on drug release from 3D printed tablets. *International journal of pharmaceutics* **494**, 2015b, 657-663.

Hirschberg, C., Edinger, M., Holmfred, E., Rantanen, J., Boetker, J., Image-Based Artificial Intelligence Methods for Product Control of Tablet Coating Quality. *Pharmaceutics* **12**, 2020.

Januszewicz, R., Mecham, S.J., Olson, K.R., Benhabbour, S.R., Design and Characterization of a Novel Series of Geometrically Complex Intravaginal Rings with Digital Light Synthesis. *Advanced Materials Technologies* **5**, 2020, 2000261.

Kadry, H., Wadnap, S., Xu, C., Ahsan, F., Digital light processing (DLP) 3D-printing technology and photoreactive polymers in fabrication of modified-release tablets. *Eur J Pharm Sci* **135**, 2019, 60-67.

Karakurt, I., Aydođdu, A., Çikrıkci, S., Orozco, J., Lin, L., Stereolithography (SLA) 3D Printing of Ascorbic Acid Loaded Hydrogels: A Controlled Release Study. *International journal of pharmaceuticals*, 2020, 119428.

Karavasili, C., Eleftheriadis, G.K., Gioumouxouzis, C., Andriotis, E.G., Fatouros, D.G., Mucosal drug delivery and 3D printing technologies: A focus on special patient populations. *Advanced Drug Delivery Reviews* **176**, 2021, 113858.

Karavasili, C., Tsongas, K., Andreadis, I.I., Andriotis, E.G., Papachristou, E.T., Papi, R.M., Tzetzis, D., Fatouros, D.G., Physico-mechanical and finite element analysis evaluation of 3D printable alginate-methylcellulose inks for wound healing applications. *Carbohydrate Polymers* **247**, 2020, 116666.

Kickstarter, 2021a. ONO - The \$99 Smartphone 3D Printer. [Online] Available at: <https://www.kickstarter.com/projects/olo3d/olo-the-first-ever-smartphone-3d-printer/description> (Accessed 23rd July).

Kickstarter, 2021b. T3D - The World's First Mobile Multifunction 3D Printer. [Online] Available at: <https://www.kickstarter.com/projects/906506734/t3d-the-worlds-first-mobile-multifunction-3d-print> (Accessed 23rd July).

Kimmel, S.E., Warfarin therapy: in need of improvement after all these years. *Expert opinion on pharmacotherapy* **9**, 2008, 677-686.

Krkobabić, M., Medarević, D., Cvijić, S., Grujić, B., Ibrić, S., Hydrophilic excipients in digital light processing (DLP) printing of sustained release tablets: Impact on internal structure and drug dissolution rate. *International journal of pharmaceuticals* **572**, 2019, 118790.

Kühnemund, M., Wei, Q., Darai, E., Wang, Y., Hernández-Neuta, I., Yang, Z., Tseng, D., Ahlford, A., Mathot, L., Sjöblom, T., Targeted DNA sequencing and in situ mutation analysis using mobile phone microscopy. *Nature communications* **8**, 2017, 1-8.

Laksanasopin, T., Guo, T.W., Nayak, S., Sridhara, A.A., Xie, S., Olowookere, O.O., Cadinu, P., Meng, F., Chee, N.H., Kim, J., A smartphone dongle for diagnosis of infectious diseases at the point of care. *Science translational medicine* **7**, 2015, 273re271-273re271.

Li, W., Wang, M., Mille, L.S., Robledo Lara, J.A., Huerta, V., Uribe Velázquez, T., Cheng, F., Li, H., Gong, J., Ching, T., Murphy, C.A., Leshia, A., Hassan, S., Woodfield, T.B.F., Lim, K.S., Zhang, Y.S., A Smartphone-Enabled Portable Digital Light Processing 3D Printer. *Adv. Mater.* **n/a**2102153.

Lim, K.S., Schon, B.S., Mekhileri, N.V., Brown, G.C., Chia, C.M., Prabakar, S., Hooper, G.J., Woodfield, T.B., New visible-light photoinitiating system for improved print fidelity in gelatin-based bioinks. *ACS biomaterials science & engineering* **2**, 2016, 1752-1762.

Lumi Industries, 2021a. LumiBee: A unique DIY resin 3D printer for smartphones. [Online] Available at: <https://www.lumindustries.com/lumibee> (Accessed

Lumi Industries, 2021b. The quest for a truly portable, high quality light-curing 3D printer. [Online] Available at: <https://www.lumindustries.com/the-new-lumifold> (Accessed 23rd July).

Madžarević, M., Ibrić, S., Evaluation of exposure time and visible light irradiation in LCD 3D printing of ibuprofen extended release tablets. *European Journal of Pharmaceutical Sciences* **158**, 2021, 105688.

- Maity, N., Mansour, N., Chakraborty, P., Bychenko, D., Gazit, E., Cohn, D., A Personalized Multifunctional 3D Printed Shape Memory - Displaying, Drug Releasing Tracheal Stent. *Advanced Functional Materials*, 2021, 2108436.
- Malas, A., Isakov, D., Couling, K., Gibbons, G.J., Fabrication of high permittivity resin composite for vat photopolymerization 3D printing: Morphology, thermal, dynamic mechanical and dielectric properties. *Materials* **12**, 2019, 3818.
- Mannino, R.G., Myers, D.R., Tyburski, E.A., Caruso, C., Boudreaux, J., Leong, T., Clifford, G., Lam, W.A., Smartphone app for non-invasive detection of anemia using only patient-sourced photos. *Nature communications* **9**, 2018, 1-10.
- Medicines & Healthcare products Regulatory Agency, 2021. Consultation on Point of Care manufacturing. [Online] Available at: <https://www.gov.uk/government/consultations/point-of-care-consultation/consultation-on-point-of-care-manufacturing> (Accessed 07/10/2021).
- Melocchi, A., Briatico-Vangosa, F., Uboldi, M., Parietti, F., Turchi, M., von Zeppelin, D., Maroni, A., Zema, L., Gazzaniga, A., Zidan, A., Quality considerations on the pharmaceutical applications of fused deposition modeling 3D printing. *Int J Pharm* **592**, 2021, 119901.
- Melocchi, A., Inverardi, N., Uboldi, M., Baldi, F., Maroni, A., Pandini, S., Briatico-Vangosa, F., Zema, L., Gazzaniga, A., Retentive device for intravesical drug delivery based on water-induced shape memory response of poly(vinyl alcohol): design concept and 4D printing feasibility. *Int J Pharm* **559**, 2019a, 299-311.
- Melocchi, A., Uboldi, M., Inverardi, N., Briatico-Vangosa, F., Baldi, F., Pandini, S., Scalet, G., Auricchio, F., Cerea, M., Foppoli, A., Maroni, A., Zema, L., Gazzaniga, A., Expandable drug delivery system for gastric retention based on shape memory polymers: Development via 4D printing and extrusion. *Int J Pharm* **571**, 2019b, 118700.
- Merchant, H.A., Goyanes, A., Parashar, N., Basit, A.W., Predicting the gastrointestinal behaviour of modified-release products: Utility of a novel dynamic dissolution test apparatus involving the use of bicarbonate buffers. *Int J Pharm* **475**, 2014, 585-591.
- Muñiz Castro, B., Elbadawi, M., Ong, J.J., Pollard, T.D., Song, Z., Gaisford, S., Pérez, G., Basit, A.W., Cabalar, P., Goyanes, A., Machine learning predicts 3D printing performance of over 900 drug delivery systems. *J. Controlled Rel.* **337**, 2021, 530-545.
- Ng, W.L., Lee, J.M., Zhou, M., Chen, Y.-W., Lee, K.-X.A., Yeong, W.Y., Shen, Y.-F., Vat polymerization-based bioprinting—process, materials, applications and regulatory challenges. *Biofabrication* **12**, 2020, 022001.
- Nguyenpho, A., Ciavarella, A.B., Siddiqui, A., Rahman, Z., Akhtar, S., Hunt, R., Korang-Yeboah, M., Khan, M.A., Evaluation of in-use stability of anticoagulant drug products: warfarin sodium. *Journal of pharmaceutical sciences* **104**, 2015, 4232-4240.
- Niese, S., Breitreutz, J., Quodbach, J., Development of a dosing device for individualized dosing of orodispersible warfarin films. *Int. J. Pharm.* **561**, 2019, 314-323.
- Oesterreicher, A., Wiener, J., Roth, M., Moser, A., Gmeiner, R., Edler, M., Pinter, G., Griesser, T., Tough and degradable photopolymers derived from alkyne monomers for 3D printing of biomedical materials. *Polymer Chemistry* **7**, 2016, 5169-5180.

Oh, H.J., Aboian, M.S., Yi, M.Y., Maslyn, J.A., Loo, W.S., Jiang, X., Parkinson, D.Y., Wilson, M.W., Moore, T., Yee, C.R., 3D printed absorber for capturing chemotherapy drugs before they spread through the body. *ACS central science* **5**, 2019, 419-427.

Oskui, S.M., Diamante, G., Liao, C., Shi, W., Gan, J., Schlenk, D., Grover, W.H., Assessing and reducing the toxicity of 3D-printed parts. *Environmental Science & Technology Letters* **3**, 2015, 1-6.

Parfenyuk, E.V., Dolinina, E.S., Development of novel warfarin-silica composite for controlled drug release. *Pharmaceutical research* **34**, 2017, 825-835.

Park, H.K., Shin, M., Kim, B., Park, J.W., Lee, H., A visible light-curable yet visible wavelength-transparent resin for stereolithography 3D printing. *NPG Asia Materials*, 2018, 1.

Paunović, N., Bao, Y., Coulter, F.B., Masania, K., Geks, A.K., Klein, K., Rafsanjani, A., Cadalbert, J., Kronen, P.W., Kleger, N., Digital light 3D printing of customized bioresorbable airway stents with elastomeric properties. *Science Advances* **7**, 2021, eabe9499.

Prendergast, M.E., Burdick, J.A., Recent advances in enabling technologies in 3D printing for precision medicine. *Advanced Materials* **32**, 2020, 1902516.

Quan, H., Zhang, T., Xu, H., Luo, S., Nie, J., Zhu, X., Photo-curing 3D printing technique and its challenges. *Bioactive Materials* **5**, 2020, 110-115.

Ragelle, H., Rahimian, S., Guzzi, E.A., Westenskow, P.D., Tibbitt, M.W., Schwach, G., Langer, R., Additive manufacturing in drug delivery: innovative drug product design and opportunities for industrial application. *Advanced Drug Delivery Reviews In Press*, 2021, 113990.

Reynolds, K.K., Valdes Jr, R., Hartung, B.R., Linder, M.W., Individualizing warfarin therapy. 2007.

Robles-Martinez, P., Xu, X., Trenfield, S.J., Awad, A., Goyanes, A., Telford, R., Basit, A.W., Gaisford, S., 3D Printing of a Multi-Layered Polypill Containing Six Drugs Using a Novel Stereolithographic Method. *Pharmaceutics* **11**, 2019, 274.

Seoane-Viaño, I., Trenfield, J.S., Basit, A.W., Goyanes, A., Translating 3D printed pharmaceuticals: from hype to real-world clinical applications. *Advanced Drug Delivery Reviews* **174**, 2021, 553-575.

Shih, H., Lin, C.C., Visible - light - mediated thiol - Ene hydrogelation using eosin - Y as the only photoinitiator. *Macromolecular rapid communications* **34**, 2013, 269-273.

Tumbleston, J.R., Shirvanyants, D., Ermoshkin, N., Januszewicz, R., Johnson, A.R., Kelly, D., Chen, K., Pinschmidt, R., Rolland, J.P., Ermoshkin, A., Continuous liquid interface production of 3D objects. *Science* **347**, 2015, 1349-1352.

Tyson, R.J., Park, C.C., Powell, J.R., Patterson, J.H., Weiner, D., Watkins, P.B., Gonzalez, D., Precision dosing priority criteria: Drug, disease, and patient population variables. *Frontiers in pharmacology* **11**, 2020, 420.

Uddin, M., Wang, Y., Woodbury-Smith, M., Artificial intelligence for precision medicine in neurodevelopmental disorders. *NPJ digital medicine* **2**, 2019, 1-10.

- Vaut, L., Juszczak, J.J., Kamguyan, K., Jensen, K.E., Tosello, G., Boisen, A., 3D printing of reservoir devices for Oral drug delivery: from concept to functionality through design improvement for enhanced Mucoadhesion. *ACS Biomaterials Science & Engineering* **6**, 2020, 2478-2486.
- Vivero-Lopez, M., Xu, X., Muras, A., Otero, A., Concheiro, A., Gaisford, S., Basit, A.W., Alvarez-Lorenzo, C., Goyanes, A., Anti-biofilm multi drug-loaded 3D printed hearing aids. *Materials Science and Engineering: C* **119**, 2021, 111606.
- Vuddanda, P.R., Alomari, M., Dodoo, C.C., Trenfield, S.J., Velaga, S., Basit, A.W., Gaisford, S., Personalisation of warfarin therapy using thermal ink-jet printing. *European Journal of Pharmaceutical Sciences* **117**, 2018, 80-87.
- Wang, J., Goyanes, A., Gaisford, S., Basit, A.W., Stereolithographic (SLA) 3D printing of oral modified-release dosage forms. *International journal of pharmaceutics* **503**, 2016, 207-212.
- Xenikakis, I., Tsongas, K., Tzimitzimis, E.K., Zacharis, C.K., Theodoroula, N., Kalogianni, E.P., Demiri, E., Vizirianakis, I.S., Tzetzis, D., Fatouros, D.G., Fabrication of hollow microneedles using liquid crystal display (LCD) vat polymerization 3D printing technology for transdermal macromolecular delivery. *International journal of pharmaceutics* **597**, 2021, 120303.
- Xenikakis, I., Tzimitzimis, M., Tsongas, K., Andreadis, D., Demiri, E., Tzetzis, D., Fatouros, D.G., Fabrication and finite element analysis of stereolithographic 3D printed microneedles for transdermal delivery of model dyes across human skin in vitro. *Eur. J. Pharm. Sci.* **137**, 2019, 104976.
- Xu, X., Awad, A., Robles-Martinez, P., Gaisford, S., Goyanes, A., Basit, A.W., Vat photopolymerization 3D printing for advanced drug delivery and medical device applications. *J. Control. Release.* **329**, 2020a, 743-757.
- Xu, X., Awwad, S., Diaz-Gomez, L., Alvarez-Lorenzo, C., Brocchini, S., Gaisford, S., Goyanes, A., Basit, A.W., 3D Printed Punctal Plugs for Controlled Ocular Drug Delivery. *Pharmaceutics* **13**, 2021a, 1421.
- Xu, X., Goyanes, A., Trenfield, S.J., Diaz-Gomez, L., Alvarez-Lorenzo, C., Gaisford, S., Basit, A.W., Stereolithography (SLA) 3D printing of a bladder device for intravesical drug delivery. *Materials Science and Engineering: C* **120**, 2021b, 111773.
- Xu, X., Robles-Martinez, P., Madla, C.M., Joubert, F., Goyanes, A., Basit, A.W., Gaisford, S., Stereolithography (SLA) 3D printing of an antihypertensive polyprintlet: Case study of an unexpected photopolymer-drug reaction. *Additive Manufacturing* **33**, 2020b, 101071.
- Yang, M.-L., Song, Y.-M., Synthesis and investigation of water-soluble anticoagulant warfarin/ferulic acid grafted rare earth oxide nanoparticle materials. *Rsc Advances* **5**, 2015, 17824-17833.
- Yang, Y., Zhou, Y., Lin, X., Yang, Q., Yang, G., Printability of External and Internal Structures Based on Digital Light Processing 3D Printing Technique. *Pharmaceutics* **12**, 2020, 207.
- Yao, W., Li, D., Zhao, Y., Zhan, Z., Jin, G., Liang, H., Yang, R., 3D Printed Multi-Functional Hydrogel Microneedles Based on High-Precision Digital Light Processing. *Micromachines* **11**, 2020, 17.

Zheng, Y., Deng, F., Wang, B., Wu, Y., Luo, Q., Zuo, X., Liu, X., Cao, L., Li, M., Lu, H., Cheng, S., Li, X., Melt extrusion deposition (MED™) 3D printing technology – A paradigm shift in design and development of modified release drug products. *Int J Pharm* **602**, 2021, 120639.